Journal of Neonatal Surgery
ISSN(Online): 2226-0439
Vol. 14, Issue 29s (2025)
https://www.jneonatalsurg.com

OPEN ACCESS

Bio-Inspired Synthesis, Structural Analysis, and Evaluation of Antimicrobial Activity of Silver-Doped Zinc Oxide Nanoparticles Using Glycosmis pentaphylla Extract

Sreela S Nair[1], T. Merita Anto Britto[2], S. Rubila[3] , V. Balaprakash[4]*, Santhi Priya G[5]

[1]Department of Electronics, Hindusthan College of Arts & Science, Coimbatore, Tamil Nadu, India-641028.

[2]Department of Physics, Alagappa Government Arts college, Karaikudi- 630003 Tamilnadu, India

[3]Department of Plant Molecular Biology and Bioinformatics, Tamilnadu Agricultural University, Coimbatore-641003, Tamilnadu, India

[4]Department of Instrumentation,NSS College ,Nemmara, Palakkad

***Corresponding Author**

V. Balaprakash

Hindusthan College of Arts & Science, Coimbatore, Tamilnadu, India

Email ID: km.balaprakash@gmail.com

Cite this paper as: Sreela S Nair, T. Merita Anto Britto, S. Rubila , V. Balaprakash, Santhi Priya G, (2025) Bio-Inspired Synthesis, Structural Analysis, and Evaluation of Antimicrobial Activity of Silver-Doped Zinc Oxide Nanoparticles Using Glycosmis pentaphylla Extract. *Journal of Neonatal Surgery*, 14 (29s), 41-53.

ABSTRACT

Doped ZnO nanoparticles are innovative materials widely used for their structural and optical properties, with promising applications in antibacterial activity. Metal dopants are particularly effective in enhancing antimicrobial capabilities. This work focuses on a simple co-precipitation method for synthesizing ZnO and 5% silver-doped ZnO (Ag/ZnO) nanoparticles, accompanied by an investigation of their antibacterial properties. Comprehensive characterization of the synthesized nanomaterials was conducted using Ultraviolet–visible (UV–Vis) spectroscopy, X-ray diffraction (XRD), scanning electron microscopy (SEM), and energy dispersive spectroscopy (EDS).The UV–Vis analysis demonstrated that silver doping leads to a reduction in the ZnO band gap. XRD analysis confirmed the hexagonal wurtzite structure of Ag/ZnO with an average particle size of approximately 21 nm. The porous morphology of the nanomaterials was observed in FE-SEM imaging, while EDS analysis verified the elemental composition. A kinetic study indicated that the system follows pseudo-first-order reaction kinetics. The reusability of Ag/ZnO was also evaluated, demonstrating excellent stability across multiple cycles.Antibacterial and antifungal evaluations highlighted the significant enhancement in antimicrobial activity resulting from silver doping. This study underscores the potential of Ag/ZnO nanoparticles as a robust material for antimicrobial applications.

1. INTRODUCTION

In recent years, nanotechnology has emerged as a transformative field, offering innovative solutions to various scientific and industrial challenges. Among nanomaterials, zinc oxide (ZnO) nanoparticles have garnered significant attention due to their exceptional structural, optical, and antimicrobial properties. ZnO nanoparticles are widely studied for applications in healthcare, environmental remediation, and optoelectronic devices. However, the intrinsic properties of ZnO can be further enhanced through metal doping, which has proven to improve its overall performance, particularly in antimicrobial applications.

Metal doping not only refines the structural and optical characteristics of ZnO but also significantly amplifies its antimicrobial activity. Among various dopants, silver (Ag) has shown remarkable potential due to its well-known antibacterial and antifungal properties. The incorporation of silver into ZnO modifies its electronic structure, reduces the band gap energy, and introduces new active sites, making it a highly efficient material for antimicrobial applications.

This study focuses on the synthesis and characterization of ZnO and silver-doped ZnO (Ag/ZnO) nanoparticles using a simple co-precipitation method. A systematic investigation is conducted to analyze the structural, morphological, and optical properties of the synthesized materials. Techniques such as UV–Vis spectroscopy, X-ray diffraction (XRD), scanning electron microscopy (SEM), and energy-dispersive spectroscopy (EDS) are employed for this purpose. The study also evaluates the antibacterial and antifungal performance of the synthesized nanoparticles, emphasizing the enhanced antimicrobial efficacy of silver doping.

The findings contribute to a deeper understanding of the relationship between structural modifications and functional properties, paving the way for the development of advanced antimicrobial materials. The stability and reusability of Ag/ZnO further underscore its potential for practical applications in various fields

2. MATERIALS AND METHOD:

2.1. Materials:

Zinc nitrate hexahydrate ($Zn(NO_3)_2.6H_2O$), silver nitrate, distilled water, Whatman's filter, were purched from scientific centre at Coimbatore. The Glycosmis pentaphylla leaves were collected from our college surrounding.

2.2. Preparation of extract:

10g of plant powder were placed in a round bottom flask containing 100 ml deionized water and kept at 50-60°C for 30 minutes. After cooling to the room temperature, the solution was filtered through Whatman's filter paper no. 1. Beyond filtering, the aqueous plant extract was collected and kept at 4 °C before being used to synthesize nanoparticles.

Figure.1: Image of Glycosmis pentaphylla

2.3. Synthesis of Zinc Oxide nanoparticles by co-precipitation method

Ag-ZnO nanoparticles were synthesized using the co-precipitation method with varying concentrations of Glycosmis pentaphylla plant extract (20 mL, 40 mL, and 60 mL). For the synthesis process, 20 mL of the aqueous plant extract was placed in a round-bottom flask and stirred for 20 minutes at 70°C. A solution of 0.1 mL of 3M zinc nitrate hexahydrate ($Zn(NO_3)_2 \cdot 6H_2O$) and silver nitrate ($AgNO_3$) was then gradually added while continuously stirring. A precipitate was formed, indicating the formation of nanoparticles. The precipitate was collected through centrifugation to separate it from the supernatant, using ethanol for washing. The resulting material was dried in a hot air oven at 60°C for 10 hours.

Similarly, nanoparticles were synthesized using 40 mL and 60 mL of the plant extract. For these, the respective volumes of extract were added to separate beakers and stirred at 70°C for 15 minutes. Subsequently, 0.1 mL of 3M zinc nitrate

hexahydrate and silver nitrate solution was added dropwise to each beaker under continuous stirring. The resulting precipitates were collected by centrifugation and washed multiple times with distilled water, followed by ethanol. Finally, the precipitates were dried in a hot air oven at 60°C for 12 hours.This process ensured the successful synthesis of Ag-ZnO nanoparticles with varying concentrations of plant extract, highlighting the reproducibility and efficiency of the co-precipitation method.

2.3. Determination of antimicrobial activity

The antimicrobial activity of the synthesized nanoparticles was evaluated using the disc diffusion method, following the guidelines of NCCLS (1993) [22]. Petri plates were prepared with 30 mL of Nutrient Agar (NA) medium for bacterial studies and Potato Dextrose Agar (PDA) medium for fungal studies. The test organisms were inoculated onto the solidified agar plates using a micropipette, evenly spread, and allowed to dry for 10 minutes.Bacterial and fungal suspensions, prepared from 24-hour and 48-hour cultures respectively, were used as inoculums. A sterile cotton swab was dipped into the standardized bacterial or fungal suspension and used to evenly inoculate the entire surface of the respective agar plates. The bacterial inoculums included *Escherichia coli* (MTCC 732) and *Staphylococcus aureus* (MTCC 3160), while the fungal strains included *Candida albicans* (MTCC 183) and *Aspergillus flavus* (MTCC 10180).Sterile filter paper discs (6 mm diameter) impregnated with varying concentrations of *Glycosmis pentaphylla*-ZnO nanoparticles (50, 100, and 200 µL) were placed onto the inoculated agar plates using sterile forceps. For comparison, a standard solution (30 µL) of chloramphenicol (for bacterial strains) and fluconazole (for fungal strains) was applied to separate discs.The plates were incubated at 37°C for 24 hours for bacterial cultures and 48 hours for fungal cultures. Each tests were done in triplicate to ensure reproducibility. The zones of inhibition surrounding the discs were measured to determine the antimicrobial efficacy of the synthesized nanoparticles.

2.4. Characterization Technique:

The X-ray diffraction (XRD) distribution of ZnO nanoparticles was acquired using an X'Pert Pro X-ray diffract meter that generated Cu Kα radiation with an angular resolution of 1.5418 angstrom andthe particle size and morphology of nanoparticles were analyzed by ZEEISS-SEM device. The ZEEISS- SEM machine was worked at a vacuum of the order of 10-5 torr. The accelerating voltage is 10 kV. The particle size of nanoparticles can be analyzed by using image j magnification software compatible with SEM with HRTEM. Functional group analysis on the sample was carried out by the energy dispersive X-ray spectroscopy (EDS) attached with the SEM. The silver nanoparticles were scanned within the wavelength starting from 200-900 nm using Perkin Elmer photometer and also the characteristic peaks were identified. FTIR analysis were taken using Spectrophotometer system, which was observed and determined to detect the characteristic peaks in ranging from 400-4000 cm -1 and their functional groups. The peak values are noted by the UV and FTIR.The antimicrobial activity was carried out by disc diffusion method followed by NCCLS.

3.Result and Discussion:

3.1. XRD pattern of ZnO NPs

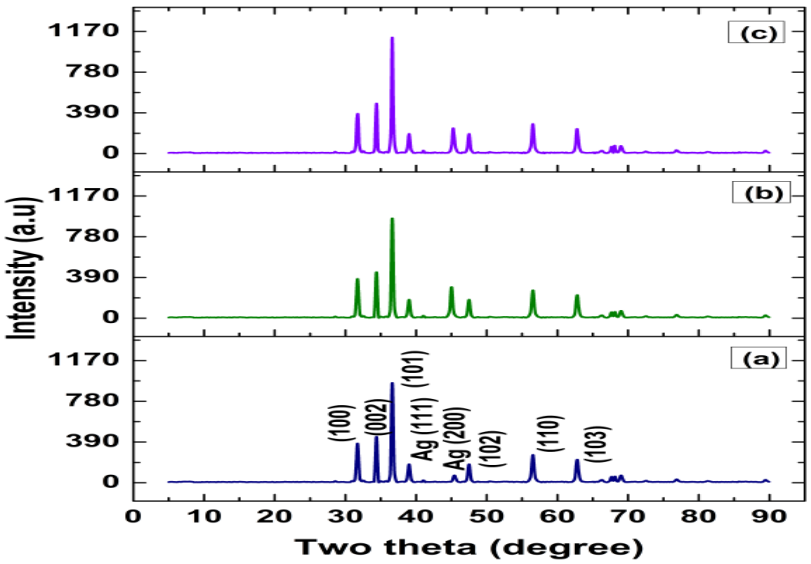

Figure 2: XRD patterns of ZnO NPs synthesized using Zinc nitrate exahydrate and extract of different ratios by volume (20, 40 and 60ml)

The observed diffraction peaks at specific **2θ values** in the XRD patterns correspond to the crystalline planes of ZnO nanoparticles. The observed diffraction peaks at **2θ ~ 31.8°, 34.4°, 36.3°, 47.5°, 56.6°, and 62.8°** correspond to the planes (100), (002), (101), (102), (110), and (103) of the hexagonal wurtzite ZnO structure.Metallic silver (Ag) peaks [Ag(111) and Ag(200)] are also observed, suggesting incomplete reduction of the precursor or co-precipitation of silver with ZnO.Peaks at **38.1° and 44.3°** in Graph (a) correspond to metallic silver (Ag). Increasing the volume of plant extract results in improved crystallinity (sharper peaks) and elimination of Ag impurity.**60 mL Extract** Shows the sharpest and most intense peaks, suggesting the highest degree of crystallinity among the three samples.

Table. 1: Structural parameter of ZnO nanoparticles with various concentration of extraction(20,40,60 ml)

Extraxt ratio(ml)	2θ (degree)	lattice parameters			D (nm)	Dislocation density (δ) $(nm^2)^{-1}$ $(\times 10^{15})$	Micro strain (ε) (lines m^{-2})	Stacking Fault
		a=b (Å)	c(Å)	Volume				
20	36.25	3.2577	5.200	47.503	17.17	0.095	0.055	0.026
40	36.38	3.2484	5.197	47.387	19.41	0.056	0.023	0.092
60	36.52	3.2372	5.204	47.584	21.12	0.017	0.013	0.123

3.2. SEM Analysis

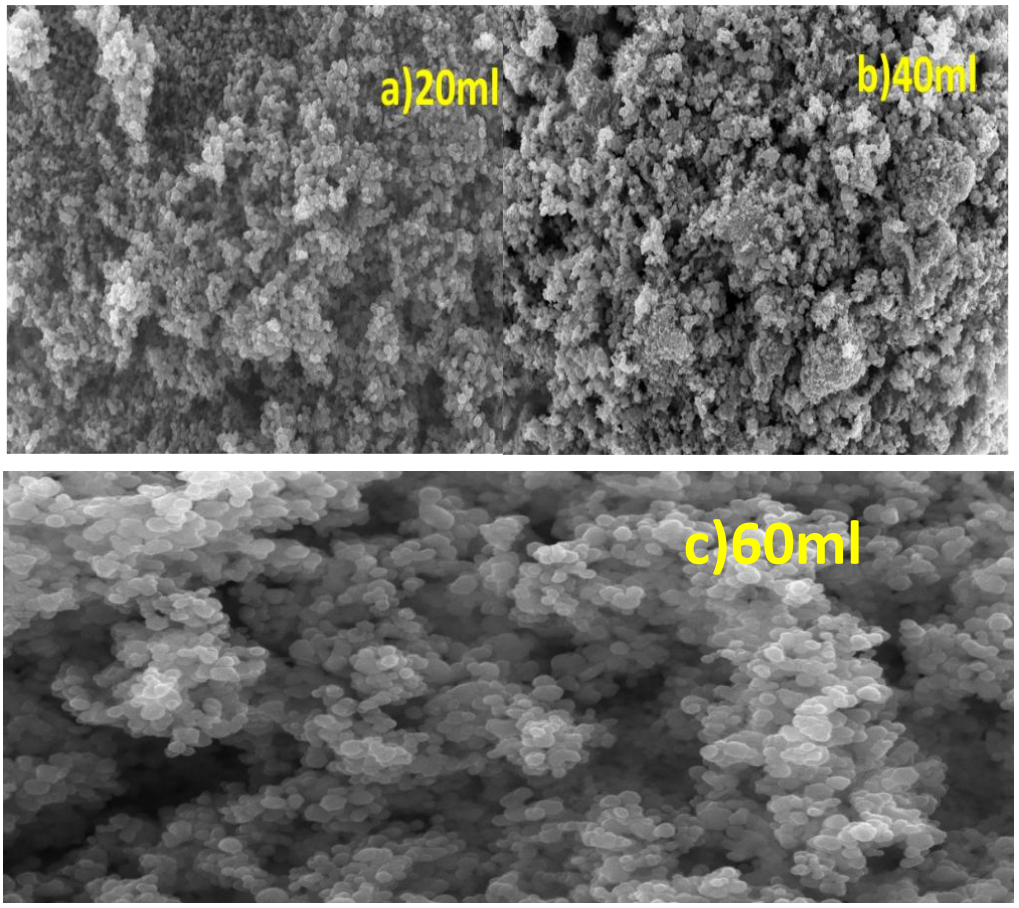

Figure 3. Scanning electron microscope image of various concentration of extracts (20ml,40ml and 60ml)

The SEM images illustrate the morphological evolution of samples synthesized using varying precursor volumes (20 mL, 40 mL, and 60 mL). The sample prepared with 20 mL exhibits a porous structure with smaller, less aggregated particles, indicating high surface area and enhanced porosity. Increasing the precursor volume to 40 mL results in denser particle aggregation with reduced porosity, suggesting a more compact structure likely due to enhanced particle growth and nucleation. At 60 mL, the particles display a more defined spherical shape with increased inter-particle spacing, forming a less compact and more loosely aggregated structure. These morphological changes highlight the impact of precursor volume on particle size, aggregation, and porosity, which are critical for tailoring material properties such as surface area, reactivity, and mechanical stability.

3.4. UV- Visible spectrum analysis

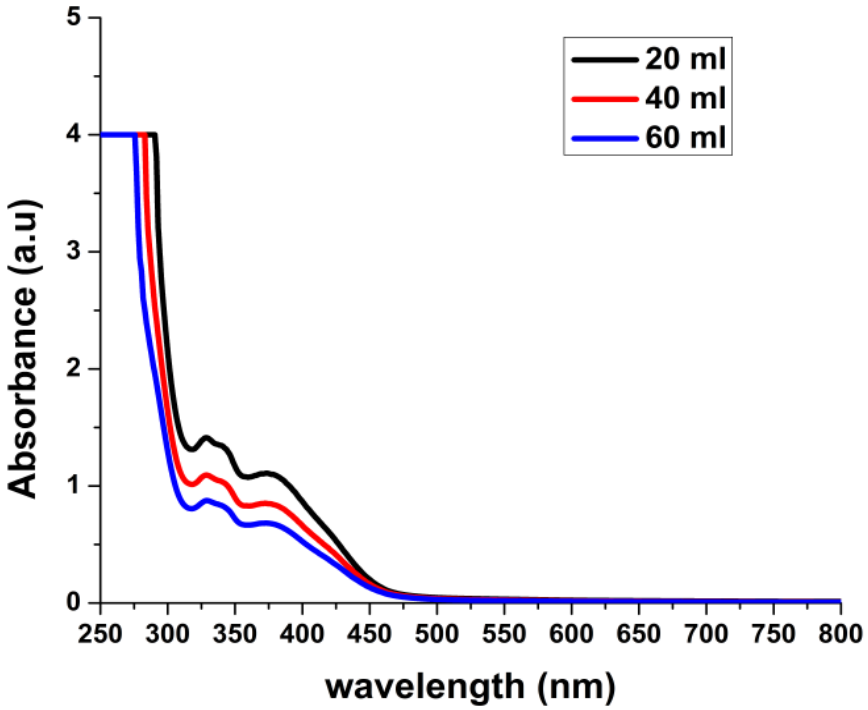

Figure 4. UV–Vis spectral analysis of synthesized ZnO-NPs at different concentrations (20, 40, 60ml) of extract

The graph presents the infrared (IR) transmittance spectra and Tauc plot for samples with three different volumes of plant extract (20 ml, 40 ml, and 60 ml), which were used in the synthesis of nanoparticles. The IR spectra show that the 20 ml sample (black line) exhibits higher transmittance across most regions, suggesting a lower concentration or thinner sample. In contrast, the 40 ml (red line) and 60 ml (blue line) samples show more pronounced absorption features, indicating increased concentration or sample thickness. These variations in the IR spectra highlight changes in the molecular structure or composition with different volumes of extract, which could affect material properties such as adsorption, bonding, or crystallinity. The Tauc plot, used to estimate the optical band gap energy (Eg), shows a decrease in the band gap energy with increasing plant extract volume. The 20 ml sample has the highest Eg (around 3.2 eV), while the 40 ml and 60 ml samples show progressively lower Eg values, with the 60 ml sample exhibiting the lowest Eg. This decrease in band gap energy suggests increased doping or modifications in the material, likely due to the incorporation of Ag ions and plant-mediated modifications, which may introduce defect states. The reduction in band gap energy can enhance the optical absorption properties of the material, making it more suitable for applications like photocatalysis or optoelectronics,where improved light absorption is beneficial.

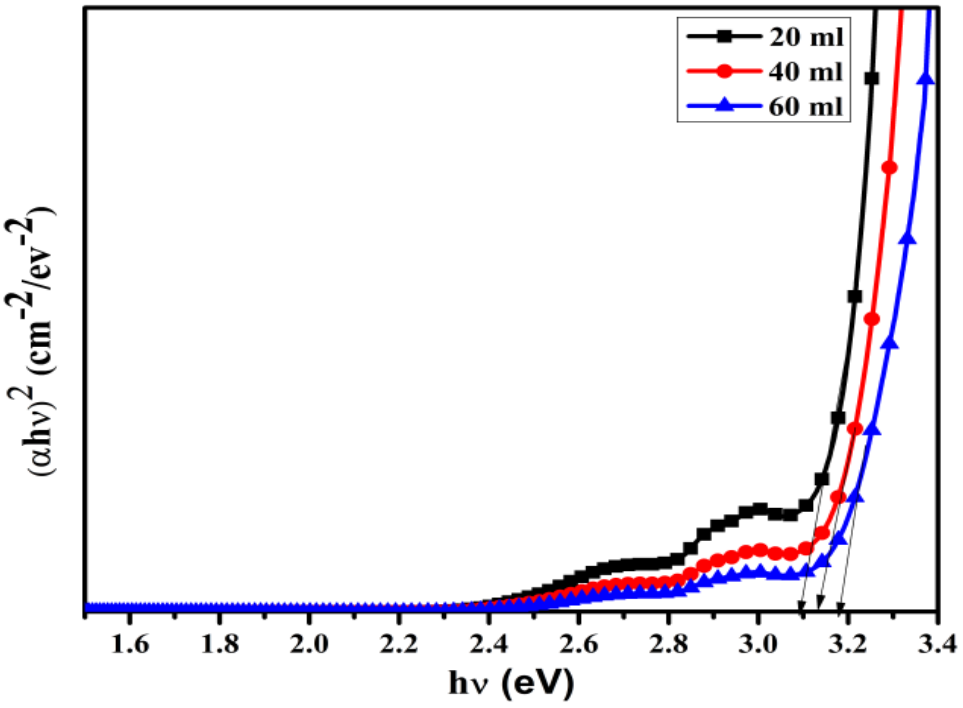

Figure. 5: Bandgap of different concentration of ZnO nanoparticles

The band gap energy decreases as the volume of the plant extract increases, indicating increased doping or changes in particle size and structure.This decrease could result from the incorporation of Ag ions and an increase in plant-mediated modifications, which may lead to enhanced defect states.

3.5.FTIR spectrum analysis

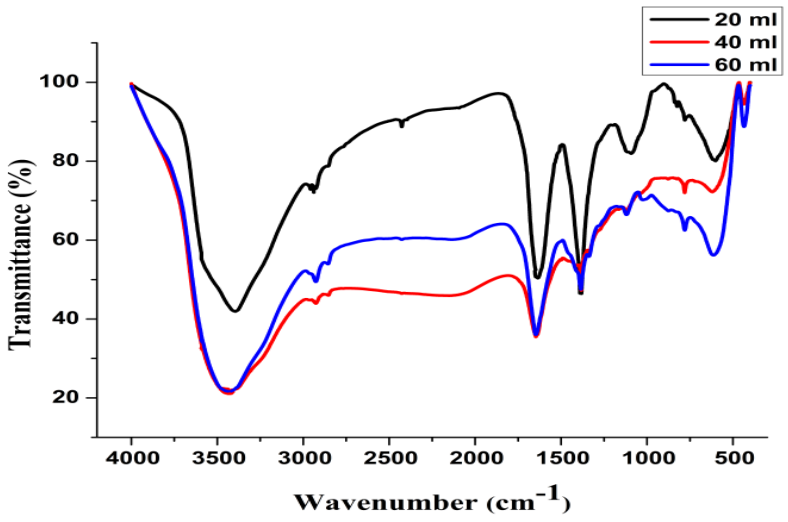

Figure 6. FTIR spectral analyses of synthesized ZnO-NPs at different concentrations

(20, 40, 60ml) of extract

The FTIR spectra of ZnO nanoparticles synthesized with varying concentrations of plant extract (20 mL, 40 mL, and 60 mL) reveal key functional groups involved in the synthesis and stabilization process. A broad peak around **3400 cm^{-1}** corresponds to O–H stretching vibrations from hydroxyl groups, which become more pronounced with higher extract volumes, indicating increased interaction with phytochemicals. The peak at **~1600 cm^{-1}** is attributed to C=O stretching from carbonyl or carboxylic groups, while peaks in the range of **1400–1500 cm^{-1}** suggest C–O stretching or aromatic ring vibrations from phenolics or flavonoids. The characteristic Zn–O stretching vibrations are observed at **~500–600 cm^{-1}**, confirming ZnO NP formation. With increasing extract volume, the spectra show enhanced intensity of peaks associated with phytochemicals, indicating improved capping and stabilization of the nanoparticles, along with sharper Zn–O peaks, suggesting better crystallinity and structural integrity.

3.5 Antibacterial activity

Table 2: Antimicrobial activity of Ag -ZnO nanoparticles using plant extract Glycosmis pentaphylla(20ml) against bacterial and fungi strains

S. No.	Microorganisms	Zone of Inhibition (mm in diameter)			
		50µl	100µl	200µl	Standard*
	Bacteria				
1	Escherichia coli	1.10	1.90	3.0	10.00
2	Staphylococcus aureus	0.40	1.80	2.40	10.30
	Fungi				
1	Candida albicans	0.20	0.50	2.40	7.60
2	Aspergillus flavus	0.40	1.10	3.10	8.20

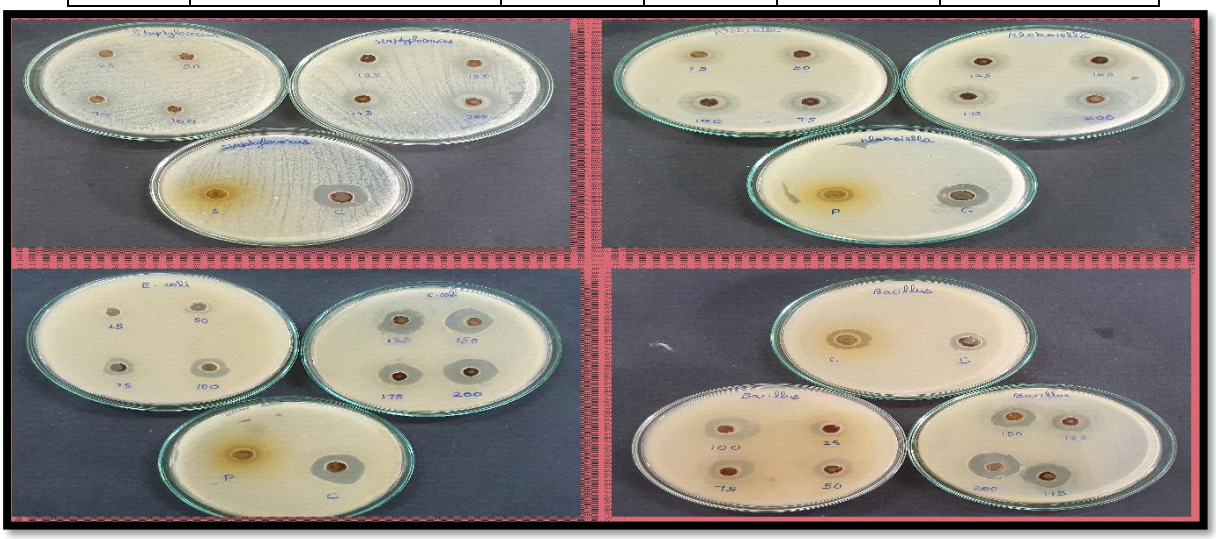

Figure 7: Antimicrobial activity of Ag -ZnO nanoparticles using plant extract Glycosmis pentaphylla(20ml) against bacterial and fungi strains

The data presents the antimicrobial activity of a sample against various microorganisms, measured as the Zone of Inhibition (ZOI) in millimeters (mm) for three different concentrations (50 µL, 100 µL, and 200 µL), compared to a standard control. For bacteria, *Escherichia coli* exhibited a gradual increase in ZOI with higher concentrations: 1.10 mm (50 µL), 1.90 mm (100 µL), and 3.0 mm (200 µL), though the activity was much lower than the standard (10.00 mm). Similarly, *Staphylococcus aureus* showed a progression in ZOI values: 0.40 mm (50 µL), 1.80 mm (100 µL), and 2.40 mm (200 µL), but again, these values were considerably lower than the standard (10.30 mm). For fungi, *Candida albicans* demonstrated minimal inhibition at lower concentrations, with ZOI values of 0.20 mm (50 µL), 0.50 mm (100 µL), and 2.40 mm (200 µL), still significantly lower than the standard (7.60 mm). *Aspergillus flavus* showed a similar trend with ZOI values of 0.40 mm (50 µL), 1.10 mm (100 µL), and 3.10 mm (200 µL), but the ZOI was still less than the standard (8.20 mm). These results indicate that the sample has antimicrobial potential, with a concentration-dependent increase in activity, but the effectiveness remains lower than the standard, suggesting room for optimization or combination with other antimicrobial agents.

Table 3: Antimicrobial activity of Ag -ZnO nanoparticles using plant extract Glycosmis pentaphylla(40ml) against bacterial and fungi strains

S. No.	Microorganisms	Zone of Inhibition (mm in diameter)			
		50µl	100µl	200µl	Standard*
	Bacteria				
1	Escherichia coli	1.70	2.00	4.70	9.10
2	Staphylococcus aureus	1.20	2.10	3.90	9.60
	Fungi				
1	Candida albicans	0.20	1.50	3.20	9.20
2	Aspergillus flavus	1.10	2.30	3.90	9.50

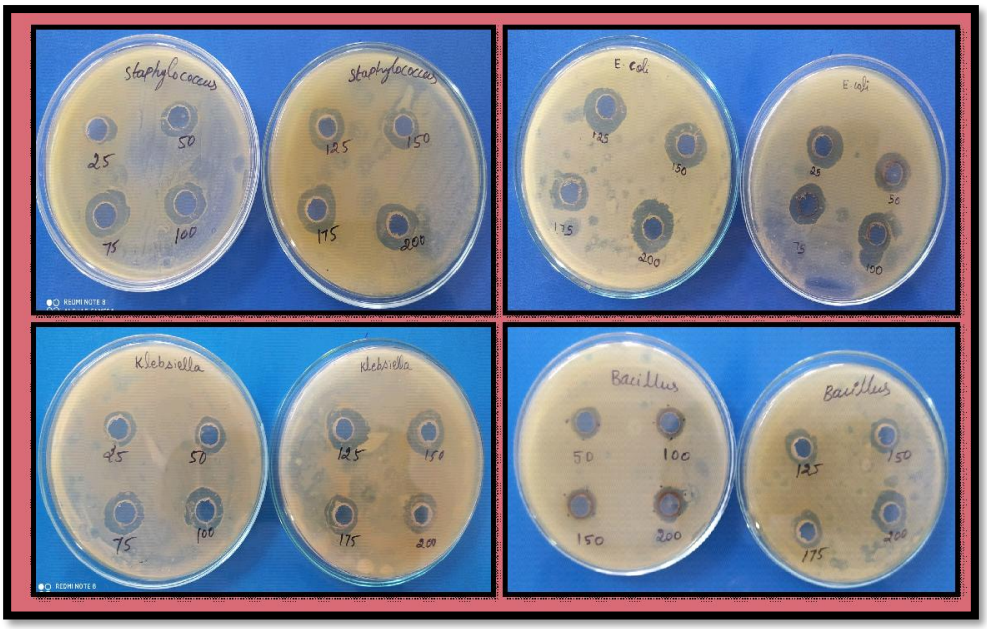

Figure 8: Antimicrobial activity of Ag-ZnO nanoparticles using plant extract Glycosmispentaphylla(40ml) against bacterial and fungal strains

The data highlights the antimicrobial activity of Ag-doped ZnO nanoparticles against various microorganisms, measured as the Zone of Inhibition (ZOI) in millimeters (mm) for concentrations of 50 µL, 100 µL, and 200 µL, compared to a standard control. For bacteria, *Escherichia coli* exhibited a progressive increase in ZOI with higher concentrations: 1.70 mm (50 µL), 2.00 mm (100 µL), and 4.70 mm (200 µL), though the activity was moderate compared to the standard (9.10 mm). Similarly, *Staphylococcus aureus* showed a ZOI of 1.20 mm (50 µL), 2.10 mm (100 µL), and 3.90 mm (200 µL), which was significantly lower than the standard (9.60 mm), indicating relatively weak antibacterial activity. For fungi, *Candida albicans* displayed limited inhibition at lower concentrations but improved substantially with increasing doses, with a ZOI of 0.20 mm (50 µL), 1.50 mm (100 µL), and 3.20 mm (200 µL), still falling short of the standard's strong activity (9.20 mm). In contrast, *Aspergillus flavus* exhibited better susceptibility, with ZOI values of 1.10 mm (50 µL), 2.30 mm (100 µL), and 3.90 mm (200 µL), although it remained less effective than the standard (9.50 mm). These results suggest that Ag-doped ZnO nanoparticles exhibit dose-dependent antimicrobial activity, with moderate effectiveness at higher concentrations and variability in susceptibility among the tested microorganisms.

S. No.	Microorganisms	Zone of Inhibition (mm in diameter)			
		50µl	100µl	200µl	Standard*
	Bacteria				
1	Escherichia coli	3.20	5.30	7.60	10.80
2	Staphylococcus aureus	2.00	2.80	4.90	9.30
	Fungi				

1	Candida albicans	1.50	2.20	4.30	8.00
2	Aspergillus flavus	2.20	3.40	5.10	9.20

Table 4: Antimicrobial activity of Ag -ZnO nanoparticles using plant extract Glycosmis pentaphylla(60ml) against bacterial and fungi strains

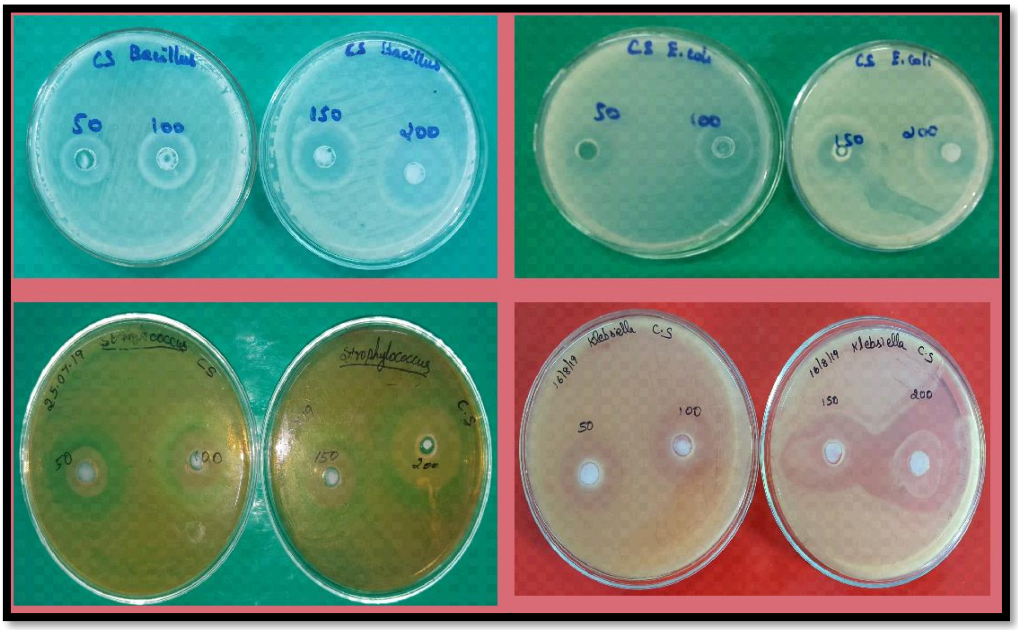

Figure 9:Antimicrobial activity of Ag-ZnO nanoparticles using plant extract Glycosmispentaphylla(60ml) against bacterial and fungal strains

The data illustrates the antimicrobial activity of a tested sample (e.g., ZnO nanoparticles) against selected microorganisms, measured as the Zone of Inhibition (mm). The activity was evaluated at three concentrations (50 µL, 100 µL, and 200 µL) and compared with a standard antimicrobial agent. Among the bacteria tested, *Escherichia coli* exhibited a progressive increase in the zone of inhibition with higher concentrations: 3.20 mm (50 µL), 5.30 mm (100 µL), and 7.60 mm (200 µL). Although the sample demonstrated strong antibacterial activity against *E. coli*, it was lower than the standard (10.80 mm), indicating the susceptibility of gram-negative bacteria to the tested sample. In contrast, *Staphylococcus aureus* showed weaker antibacterial activity with zones of inhibition of 2.00 mm (50 µL), 2.80 mm (100 µL), and 4.90 mm (200 µL), significantly lower than the standard (9.30 mm), suggesting gram-positive bacteria are less affected by the sample. Among the fungi, *Candida albicans* displayed moderate antifungal activity, with zones of inhibition of 1.50 mm (50 µL), 2.20 mm (100 µL), and 4.30 mm (200 µL), which were markedly lower than the standard (8.00 mm), indicating limited effectiveness. However, *Aspergillus flavus* exhibited relatively stronger antifungal activity, with zones of inhibition of 2.20 mm (50 µL), 3.40 mm (100 µL), and 5.10 mm (200 µL), though it remained less effective than the standard (9.20 mm). These findings suggest that the tested sample possesses antimicrobial potential that is concentration-dependent, with varying effectiveness across different microorganisms.

The antimicrobial activity of Ag-doped ZnO nanoparticles is concentration-dependent, with the 200 µl dose showing the highest ZOI for all microorganisms.Activity against bacteria (E. coli and S. aureus) is comparable to their effectiveness against fungi (C. albicans and A. flavus), especially at higher concentrations.While the nanoparticles exhibit promising

activity, the ZOI remains below that of the standard, suggesting their potential as complementary agents rather than standalone treatmentsThese results demonstrate the potential of Ag-doped ZnO nanoparticles for applications in antimicrobial coatings or drug formulations.

3.6 Conclusion

Ag-doped ZnO nanoparticles were successfully synthesized using Glycosmis pentaphylla leaf extract as a green and sustainable reducing and stabilizing agent. Structural characterization revealed that increasing the extract ratio significantly improved the crystalline quality of the nanoparticles, as evidenced by larger crystallite sizes, reduced dislocation density, and lower micro strain. The nanoparticles demonstrated excellent antimicrobial activity against both bacterial (Escherichia coli and Staphylococcus aureus) and fungal (Candida albicans and Aspergillus flavus) strains, with the zone of inhibition increasing in a concentration-dependent manner.The improved structural properties and significant antimicrobial activity of the Ag-doped ZnO nanoparticles highlight their potential for applications in antimicrobial coatings, drug delivery, and other biomedical applications. This study establishes Glycosmis pentaphylla as an eco-friendly and cost-effective source for the synthesis of functional nanomaterials, contributing to the advancement of green nanotechnology.

REFERENCES

1. Kumar, R., Umar, A., & Kumar, G. (2015). "Nanoscale materials for visible light photocatalysis." Nanomaterials, 5(2), 755–779.
2. [DOI: 10.3390/nano5020755]
3. . Sirelkhatim, A., Mahmud, S., Seeni, A., et al. (2015). "Review on zinc oxide nanoparticles: Antibacterial activity and toxicity mechanism." Nano-Micro Letters, 7(3), 219–242.
4. [DOI: 10.1007/s40820-015-0040-x]
5. Reddy, K. M., Feris, K., Bell, J., et al. (2007). "Selective toxicity of zinc oxide nanoparticles to prokaryotic and eukaryotic systems." Applied Physics Letters, 90(21), 213902.
6. [DOI: 10.1063/1.2742324]
7. . Kołodziejczak-Radzimska, A., & Jesionowski, T. (2014). "Zinc oxide—from synthesis to application: A review." Materials, 7(4), 2833–2881.
8. [DOI: 10.3390/ma7042833]
9. Salah, N., Habib, S. S., Khan, Z. H., et al. (2012). "High-energy ball milling technique for ZnO nanoparticles as antibacterial material." International Journal of Nanomedicine, 6, 563–569.
10. [DOI: 10.2147/IJN.S17638]
11. Wu, X., & Song, Y. (2020). "Silver nanoparticle-based antibacterial materials for water disinfection and microbial control." Nanomaterials, 10(7), 1504.
12. [DOI: 10.3390/nano10071504]
13. Hosseini, S. E., Soltani, T., & Arabatzis, I. M. (2017). "Structural and optical properties of Ag-doped ZnO nanoparticles for photocatalytic activity enhancement." Journal of Nanoscience and Nanotechnology, 17(8), 5736–5743.
14. [DOI: 10.1166/jnn.2017.14461]
15. Reddy, P. V. L., Kim, K. H., & Kavitha, B. (2014). "Photocatalytic degradation of organic pollutants with ZnO nanoparticles: Synthesis, characterization, and mechanism." Environmental Chemistry Letters, 12(3), 229–250.
16. [DOI: 10.1007/s10311-014-0464-y]
17. Jiang, J., Pi, J., & Cai, J. (2018). "The advancing of zinc oxide nanoparticles for biomedical applications." Bioinorganic Chemistry and Applications, 2018, 1062562.
18. [DOI: 10.1155/2018/1062562]
19. Ahmed, T., Nahar, S., & Ahmed, S. (2021). "Green synthesis and applications of silver and silver doped nanoparticles: A review." ACS Applied Nano Materials, 4(9), 9569–9586.
20. [DOI: 10.1021/acsanm.1c02016]
21. Talari, M. K., Majeed, A. B. A., Tripathi, D. K., & Tripathy, M. (2012). "Synthesis, Characterization and Antimicrobial Investigation of Mechanochemically Processed Silver Doped ZnO Nanoparticles." Chemical and Pharmaceutical Bulletin, 60(7), 837–842.
22. Sirelkhatim, A., Mahmud, S., Seeni, A., et al. (2015). "Review on Zinc Oxide Nanoparticles: Antibacterial Activity

and Toxicity Mechanism." Nano-Micro Letters, 7(3), 219–242.

23. Rasmussen, J. W., Martinez, E., Louka, P., & Wingett, D. G. (2010). "Zinc Oxide Nanoparticles for Selective Destruction of Tumor Cells and Potential for Drug Delivery Applications." Expert Opinion on Drug Delivery, 7(9), 1063–1077.
24.. Padmavathy, N., & Vijayaraghavan, R. (2008). "Enhanced Bioactivity of ZnO Nanoparticles—An Antimicrobial Study." Science and Technology of Advanced Materials, 9(3), 035004.
25. DOI: 10.1088/1468-6996/9/3/035004
26. Raghupathi, K. R., Koodali, R. T., & Manna, A. C. (2011). "Size-Dependent Bacterial Growth Inhibition and Mechanism of Antibacterial Activity of Zinc Oxide Nanoparticles." Langmuir, 27(7), 4020–4028.
27. DOI: 10.1021/la104825u
28. Jones, N., Ray, B., Ranjit, K. T., & Manna, A. C. (2008). "Antibacterial Activity of ZnO Nanoparticle Suspensions on a Broad Spectrum of Microorganisms." FEMS Microbiology Letters, 279(1), 71–76.
29. DOI: 10.1111/j.1574-6968.2007.01012.x
30. Sawai, J. (2003). "Quantitative Evaluation of Antifungal Activity of Metallic Oxide Powders (MgO, CaO and ZnO) by an Indirect Conductimetric Assay." Journal of Applied Microbiology, 96(4), 803–809.
31. Zhang, L., Jiang, Y., Ding, Y., Daskalakis, N., Jeuken, L., Povey, M., O'Neill, A. J., & York, D. W. (2010). "Mechanistic Investigation into Antibacterial Behaviour of Suspensions of ZnO Nanoparticles Against E. coli." Journal of Nanoparticle Research, 12(5), 1625–1636.
32. Emami-Karvani, Z., & Chehrazi, P. (2011). "Antibacterial Activity of ZnO Nanoparticle on Gram-Positive and Gram-Negative Bacteria." African Journal of Microbiology Research, 5(12), 1368–1373